Growth of titanium nitride: From clusters to microcrystals

Z. Y. Chen and A. W. Castleman

Citation: J. Chem. Phys. **98**, 231 (1993); doi: 10.1063/1.464669
View online: http://dx.doi.org/10.1063/1.464669
View Table of Contents: http://jcp.aip.org/resource/1/JCPSA6/v98/i1
Published by the American Institute of Physics.

Growth of titanium nitride: From clusters to microcrystals

Z. Y. Chen and A. W. Castleman, Jr.
Department of Chemistry, The Pennsylvania State University, University Park, Pennsylvania 16802

(Received 17 August 1992; accepted 14 September 1992)

Time-of-flight mass spectrometry is used to investigate $(TiN)_n^+$ clusters produced by a laser-induced plasma reactor source. The mass spectral abundance patterns indicate that the clusters have cubic structures resembling subunits of the fcc lattice of solid TiN. The primary stoichiometries observed are $(TiN)_n^+$ ($n=1$–126), except for $Ti_nN_{n-1}^+$ ($n=14$, 63). The most stable structures of the clusters are cuboids, in some cases containing a completed terrace. Even at the very early stages of crystal growth, the gas-phase clusters prefer a cubic crystalline atomic arrangement with a highly symmetric structure.

I. INTRODUCTION

Investigations of the formation and properties of clusters provide a valuable way of following the molecular details of the changing course of a system from the gaseous to the condensed state.[1–3] When studies are performed on species in the gas phase, mass-spectrometric techniques make it possible to identify the constituents of the comparatively stable clusters. This enables investigation of the growth patterns and properties of the clusters as a function of composition and degree of aggregation, serving to bridge the gap between the isolated atom or molecule on the one hand and condensed matter on the other.

In general, the structures and dynamics of atomic clusters are currently better understood than those comprised of molecular constituents.[4–7] In the past decade, considerable attention has been directed to studies of the transition from the monomer to the condensed state for systems consisting of atoms such as rare gases and metals. For molecular systems, however, the study of this transition is more demanding, owing to the complexity of the electronic structure of the subunits.

In terms of the development of molecular solids, there are comparatively few molecular cluster systems that have been well studied in the gas phase by mass spectrometry with the objective of understanding this transition. One such successful example is the study of the evolving structure of alkali-halide clusters. It is found in the gas phase that as these clusters become progressively larger, they prefer NaCl crystal atomic arrangements.[8–10] Clusters having the form of a rectangular solid are particularly stable, even if the number of positive and negative ions are not equal. In further studies of this system, Honea, Homer, and Whetten[11] observed three types of positively charged sodium chloride clusters: the purely ionic form, the excess-electron form, and the excess-hole form. The nature of the phase transformation in small alkali-halide clusters has also been investigated using molecular-dynamic simulations.[12,13] It is concluded that for small clusters, distinct, diffusionless isomerization occurs. Intermediate-size clusters exhibit hierarchial kinetics with isomerization proceeding at the onset of diffusion and melting. Well-defined, sharp-melting transitions and solid–liquid coexistence are found only for relatively large clusters. Ziemann and Castleman[14–16] also carried out a series of studies on alkali-earth metal-oxide clusters. The abundance patterns of singly and doubly charged clusters $(MO)_n^+$, $(MO)_nM^+$, and $(MO)_nM^{2+}$ (here M=Ca, Mg) showed that the clusters have cubic structures, resembling pieces of the MO fcc crystal lattice.

Transition-metal carbides and nitrides continue to be of considerable practical and theoretical interest. This class of substance exhibits, on the one hand, high melting points and ultrahardness—properties typical of covalent compounds—and, on the other hand, metallic properties, such as good electrical and thermal conductivity. For example, TiN shows an unusually high hardness and melting point.[17] (According to Mohs's scale, on which that of diamond is 10, the hardness of TiN is 8–9, and its melting point is 3220 K.) Electronic structure theory shows that stoichiometric and substoichiometric TiN crystallizes in the sodium chloride structure, and that all three main types of chemical bonding occurs; that is, metallic bonding, ionic bonding, and covalent bonding.[18] Hence, a characterization of the binding features of $(TiN)_n^+$ clusters, particularly a study of changes in the geometric structural patterns with n, would represent a valuable step towards understanding the electronic structure and chemical bonding of this system.

In this article we report results of our recent studies on TiN clusters in a time-of-flight mass spectrometer. The clusters are produced by a unique technique[19–21] involving a laser-induced plasma dehydrogenation reaction. The TiN subunit in the clusters is of a different binding character than that of any known alkali-halide or alkali-earth-oxide cluster. NaF and MgO are typical ionically bonded compounds, while TiN has considerable covalent bond character. The difference of the elemental electronegativities between the negative and positive ion is 1.5 in Pauling's scale for TiN, compared with 3.05 for NaF and 2.13 for MgO.[22] Therefore, it is interesting to compare their aggregational behavior. Additionally, TiN represents one member of a class of important electronic materials, namely the transition-metal nitrides. Information about their chemical binding, nucleation pathway, and building blocks during crystal growth bears on the importance of their synthesis and applications.

 0021-9606/93/010231-5$06.00

II. EXPERIMENT

The details of the photoionization time-of-flight (TOF) apparatus will be described in detail elsewhere.[23] Only those parts of the apparatus that relate to the results reported herein are briefly described. A pulsed supersonic neutral TiN cluster beam is generated via a laser-induced plasma reactor source, modified from a laser vaporization source.[24,25] The frequency-doubled output of a focused Nd:YAG laser (Spectra-Physics DCR-1) is focused onto a titanium metal rod with a typical power of 10 mJ/pulse. The high-temperature plasma, which contains ions and neutral metal atoms, is carried in a supersonic gas jet produced by pulsing high-pressure He (ca. 6 atm) over the metal rod. The carrier gas is previously mixed with a 200 torr partial pressure of ammonia gas (anhydrous, Linde). Titanium nitride clusters are formed once the energetic plasma, which surges from the surface of the rod, undergoes reaction with the ammonia molecules (99.99%, Johnson Matthey). These clusters are thermalized by the He buffer gas. Then they are cooled further to a low temperature in the subsequent supersonic expansion, effected into vacuum through a conical-shaped nozzle. After the supersonic jet is skimmed at the end of the main expansion chamber, it enters the ionization chamber. Photoionization is accomplished with a fixed-energy photon from the frequency-tripled output of a second Nd:YAG laser (Spectra-Physics GCR-3) utilizing a typical fluence of 10 mJ/cm^2. The cluster ions thus produced are then mass analyzed in the TOF mass spectrometer. This mass spectrometer contains a double-acceleration region followed by a long field-free region, according to the design of Wiley and McLaren.[26] The ions are detected with a multichannel plate located at the end of the flight path, and the signal is collected in a digital storage oscilloscope (LeCroy 9400A). The lasers, pulsed valve driver, and the oscilloscope are all synchronized through a multichannel delay generator. The experimental control and data acquisition are accomplished with a PC.

III. RESULTS AND DISCUSSION

A. Production of TiN clusters

The details of the mechanism of the formation of TiN cluster formation are still not completely understood. However, experiments show this technique can be used in the preparation of a wide variety of transition-metal carbide, nitride, oxide, and silicide binary compounds. This can be accomplished by introducing hydrogen-containing molecules, such as C_2H_4, NH_3, H_2O, and SiH_4, respectively, into the carrier gas. A preliminary explanation is that the high-temperature plasma produced from irradiating the metal rod causes dehydrogenation of those molecules. The nascent C, N, O, and Si atoms react with metal atoms that surge from the rod surface to form binary clusters.[20,21] The production of $(TiN)_n$ can be expressed by the following equation:

$$NH_3(g) + Ti(\text{rod}) + h\nu \rightarrow (TiN)_n . \quad (1)$$

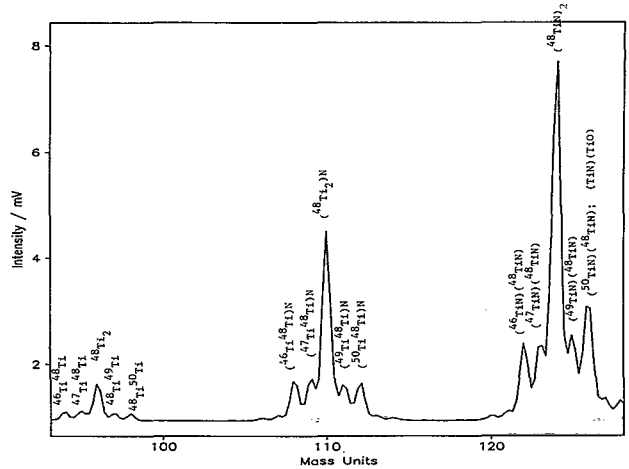

FIG. 1. TOF mass spectrum of $(TiN)_n^+$ clusters produced by a laser-induced plasma reactor source. Ionization of the neutral clusters is accomplished by photoionization with a third harmonic of a YAG laser (355 nm). The assignments of cluster ion peaks Ti_2^+, Ti_2N^+, and $Ti_2N_2^+$ are validated by their isotope patterns: ^{46}Ti 8.0%, ^{47}Ti 7.3%, ^{48}Ti 73.8%, ^{49}Ti 5.5%, and ^{50}Ti 5.4%. The high abundance of mass peak of $(^{50}TiN)(^{48}TiN)^+$ at 126 amu is attributed to the impurity of $(TiN)(TiO)^+$.

Figures 1–3 show the photoion intensity of TiN clusters obtained by ionization of neutral TiN clusters. Ionization is accomplished by multiphoton ionization with the third harmonic of a Nd:YAG laser (355 nm). The actual neutral cluster distributions are likely to be different from the observed ion distributions. This is because the intensity of a given species in a mass spectrum is influenced by many factors. Some of the important ones are the cross section for ionization of the neutral clusters, the stability of the ionized clusters, and the photofragmentation of the photoions. However, in many cases, the ion distribution does qualitatively reflect the neutral distribution provided that

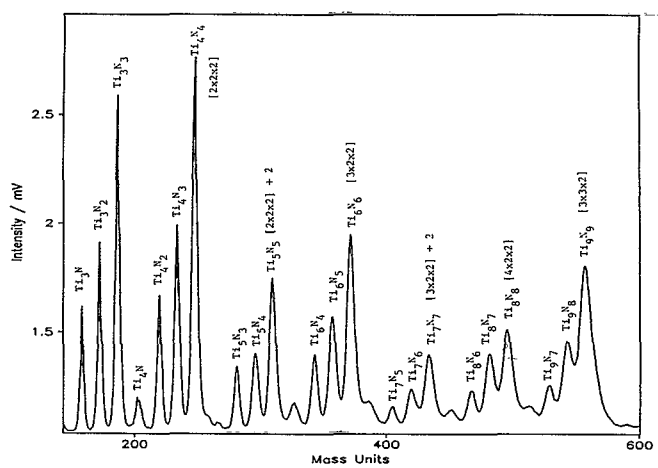

FIG. 2. TOF mass spectrum of $(TiN)_n^+$ clusters produced by a laser-induced plasma reactor source. Ionization of the neutral clusters is accomplished by photoionization with a third harmonic of a YAG laser (355 nm). There are at least three cluster series exist in the mass spectra, $(TiN)_n^+$, $Ti_nN_{n-1}^+$, and $Ti_nN_{n-2}^+$ series. Some $Ti_nN_{n-3}^+$ are also observed such as Ti_4N^+ and $Ti_6N_3^+$. It is surprising to see that a NaCl lattice structure actually occurs at the very early stages of clustering.

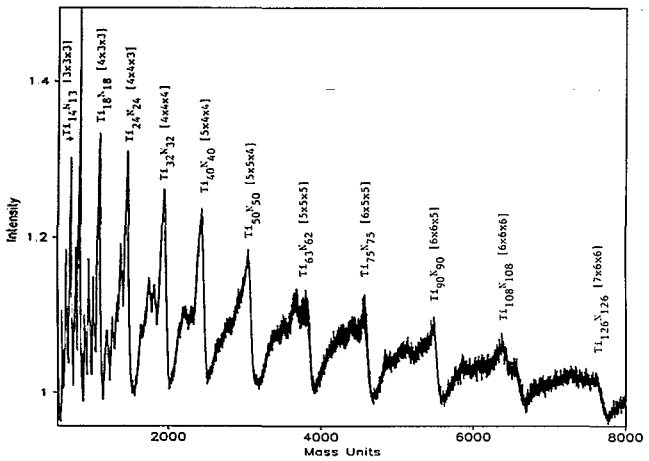

FIG. 3. TOF mass spectrum of $(TiN)_n^+$ clusters produced by a laser-induced plasma reactor source. Ionization of the neutral clusters is accomplished by photoionization with a third harmonic of a YAG laser (355 nm). The mass spectral abundance patterns indicate that the clusters have cubic structures resembling pieces of the fcc lattice of solid TiN. $Ti_{14}N_{13}^+$ are magic peaks, but not $Ti_{14}N_{14}^+$ or $Ti_{13}N_{13}^+$, whereby the lattice structure of $[3\times3\times3]$ is accommodated. This high-symmetry structure is expected to be much more stable than the other ions in local proximity.

the photoionization laser power is not so high as to cause severe fragmentation.

In Fig. 1, the cluster ion peaks Ti_2^+, Ti_2N^+, and $Ti_2N_2^+$ are clearly displayed. Their assignments are validated by their isotope patterns. Ti consists of five stable isotopes with natural abundances:[27] ^{46}Ti 8.0%, ^{47}Ti 7.3%, ^{48}Ti 73.8%, ^{49}Ti 5.5%, and ^{50}Ti 5.4%. The mass peak of $(^{50}TiN)(^{48}TiN)^+$ at 126 amu has an apparent higher abundance than expected from the isotope abundance ratio. It can be attributed to the impurity of $(TiN)(TiO)^+$. Trace amounts of oxygen can come from either the He carrier gas or the ammonia gas introduced into the plasma reactor.

B. $(TiN)_n^+$, $Ti_nN_{n-1}^+$, and $Ti_nN_{n-2}^+$ series

From Figs. 1 and 2, it is clear that there are at least three cluster series that exist in the mass spectra: the $(TiN)_n^+$ series that contains equal numbers of the metal cation and nitrogen anion, and the $Ti_nN_{n-1}^+$ and $Ti_nN_{n-2}^+$ series. The last two series contain one and two fewer anion components, respectively. Some $Ti_nN_{n-3}^+$ series are also observed such as Ti_4N^+ and $Ti_6N_3^+$ in Fig. 2. These series are also expected to exist in higher-order clusters. However, they cannot be assigned in Fig. 3 due to the limitation of the mass spectrometer's resolution used in this experiment. These three cluster series also were observed in alkali-halide clusters. Each of them corresponds to a distinct physical situation.[11] $(TiN)_n^+$ is of the excess-hole form, $Ti_nN_{n-1}^+$ the ionic form, and $Ti_nN_{n-2}^+$ is of the excess-electron form. The concurrence of $(TiN)_n^+$, $Ti_nN_{n-1}^+$, and Ti_nN_{n-2} suggests a fragmentation process in multiphoton ionization:

$$
\begin{aligned}
&(TiN)_m + rh\nu \rightarrow (TiN)_n + (m-n)(TiN)\\
&\qquad\qquad\quad sh\nu \downarrow\\
&\qquad\qquad (TiN)_n^+ + N\\
&\qquad\qquad\quad \downarrow\\
&\qquad\qquad (Ti_nN_{n-1})^+ + N\\
&\qquad\qquad\quad \downarrow\\
&\qquad\qquad (Ti_nN_{n-2})^+ + N. \qquad (2)
\end{aligned}
$$

Here a neutral cluster $(TiN)_m$ absorbs r photons and fragments to $(TiN)_n$ with a favorable geometric structure, losing $m-n$ units of TiN. The $(TiN)_n$ then absorbs another s photons and ionizes to $(TiN)_n^+$. Some of the $(TiN)_n^+$ molecules further fragment to $(Ti_nN_{n-1})^+$ and $(Ti_nN_{n-2})^+$. The role of cluster temperature on desorption of neutral atoms has been experimentally confirmed to be very sensitive to the internal energy of the cluster. For example, Pflaum, Sattler, and Recknagel[28] did observe that the electron-impact ionization of cold clusters generated $(NaCl)_n^+$, whereas ionization of warm clusters generated $Na_nCl_{n-1}^+$ ions only. According to a multiphoton stimulated desorption mechanism,[28] when the cluster is cold, $m-n$ TiN units desorb from neutral $(TiN)_m$ clusters before ionization [as indicated in the first step of Eq. (2)]. In contrast, for the warm neutral clusters, the neutral adatoms N instead of TiN can desorb from the cluster. The third step in Eq. (2) proceeds the ionization step. In our experimental work, we employ an extension nozzle to enhance clustering and cooling of the cluster beam, so the clusters are expected to be internally quite cold. Also, our multiphoton ionization laser is intentionally unfocused, which reduces the possibility of photofragment. As a result of these experimental conditions, the $(TiN)_n^+$ cluster series is much stronger than that of $(Ti_nN_{n-1})^+$ and $(Ti_nN_{n-2})^+$. This suggests that the clusters observed here may be cooler than the alkali-halide clusters in the experiments of Honea, Homer, and Whetten, where $(Na_nF_{n-1})^+$ clusters were found to be the most energetically favorable species.

Another significance of the observation of the dominating $(TiN)_n^+$ series is that we are likely to probe the neutral $(TiN)_n$ cluster abundances, but not the ionic species. The $(TiN)_n^+$ cluster series mainly reflect the abundance of the specific neutral cluster $(TiN)_n$. While in the $(Ti_nN_{n-1})^+$ or $(Ti_nN_{n-2})^+$ series, the ions are the product of the ionization of neutral clusters. They are the fragments of the parent ions. Their abundance patterns are less informative because the stability and the internal energy of the parent ions play a role in determining their abundance patterns in the mass spectra.

C. Proposed structure of $(TiN)_n$ cluster

The structures of the $(TiN)_n$ clusters can now be addressed. Both experiment and electronic structure theory show that stoichiometric and substoichiometric TiN crystallizes in a sodium chloride structure.[18] Table I summarizes the clusters that exhibit local maxima in the mass spectral of $(TiN)_n^+$ clusters. The proposed cuboid struc-

TABLE I. Magic numbers in $(TiN)_n^+$ cluster and their proposed structures.

Structure	$(TiN)_n^+$	$(Ti_nN_{n-1})^+$	Structure	$(TiN)_n^+$	$(Ti_nN_{n-1})^+$
[2×2×1]	2		[4×4×4]	32	
[3×2×1]	3		[5×4×4]	40	
[2×2×2]	4		[5×5×4]	50	
[3×2×2]	6		[5×5×5]		63
[3×3×2]	9		[6×5×5]	75	
[3×3×3]		14	[6×6×5]	90	
[4×3×3]	18		[6×6×6]	108	
[4×4×3]	24		[7×6×6]	126	

tures corresponding to the numbers of ions along the x, y, and z axes are listed in the first column. The number of TiN units in the clusters observed experimentally is listed in the second and third columns. Some proposed structures of these cluster ions are displayed in Figs. 4 and 5; the solid circle represents the Ti atom and the open circle represents the N atom.

In the early stages of the clustering process, every time a new atom or molecule (in this case, the TiN unit) condenses onto a cluster, the atoms in the cluster completely rearrange themselves to achieve a geometric structure with a minimum energy. After a cluster reaches a certain size, it is no longer free to reconstruct each time a new atom or molecule is added. A final lattice structure becomes frozen into a cluster. At this stage, clusters can be called a microcrystal. From the experimental results shown in Figs. 2 and 3, it is surprising to see that the fcc NaCl lattice structure actually occurs at a very early stage of clustering. In other words, even very small sizes of TiN clusters also prefer a cuboid structure. For example, the magic peaks at $Ti_4N_4^+$ and $Ti_9N_9^+$ indicate the stability of the [2×2×2] and [3×3×2] structures. One of the striking features about the building patterns is that $Ti_{14}N_{13}^+$ is a magic peak, but not $Ti_{14}N_{14}^+$ or $Ti_{13}N_{13}^+$. This evidently is due to the accommodation of a lattice structure of [3×3×3]. Another observed fact is that $Ti_{63}N_{62}^+$ is a magic peak, but not $Ti_{63}N_{63}^+$ or $Ti_{62}N_{62}^+$, again evidently in order to accommodate a lattice structure of [5×5×5]. These two structures are of high symmetry and without a permanent dipole moment. They can be expected to be much more stable than the other proximate species, even though the number of cations does not equal the number of anions in the cluster. The analogous compounds in the alkali-halide clusters $Na_{14}F_{13}^+$, $Na_{14}Cl_{13}^+$ also show unusual stability.[28] This is a good example that the geometric structure rather than the electronic structure plays a major role in influencing the pathway along which these classes of molecules evolve from a cluster to a crystal.

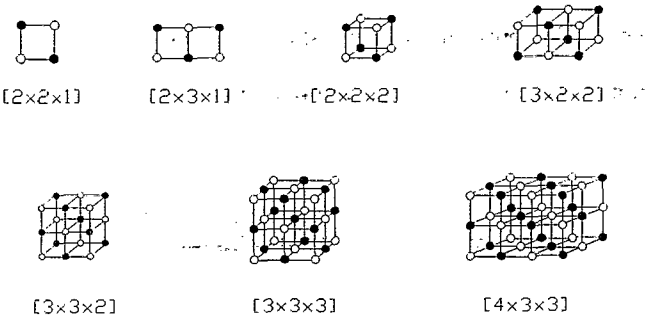

FIG. 4. Proposed structures of $(TiN)_n^+$ clusters, based on magic numbers observed in mass spectra. The solid circle represents the Ti atom and the open circle represents the N atom. Note that in the [3×3×3] structure the number of Ti atoms is not equal to the number of N atoms. See the text for a discussion of this point.

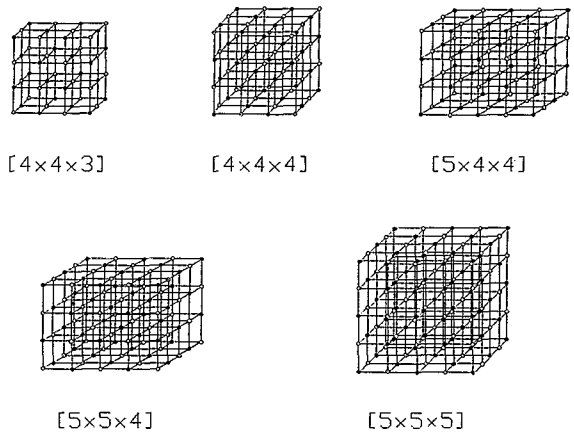

FIG. 5. Proposed structures of $(TiN)_n^+$ clusters, based on magic numbers observed in mass spectra. The solid circle represents the Ti atom and the open circle represents the N atom.

There are two other types of structures which can be derived from the perfect lattice structures shown in Figures 4 and 5. First, the $Ti_nN_{n-1}^+$ and $Ti_nN_{n-2}^+$ cluster series contain one and two less nitrogens, which can be accommodated with a structure where one or two vacancies occur in the lattice. Second, some of the clusters can have cubic structures with one dangling TiN unit on the edge of the lattice. For instance, $Ti_5N_5^+$ evidently has a structure [2×2×2]+2 with an additional TiN unit dangling on a [2×2×2] cubic lattice. In addition, $Ti_7N_7^+$ apparently has a structure [3×2×2]+2 with an extra TiN unit located on a [3×2×2] cubic lattice. Figure 6 shows these two cases.

D. Comparing TiN clusters to ultrafine particles of TiN

It is very interesting to consider the similarity of large TiN clusters and ultrafine particles of TiN produced by evaporating Ti in an atmosphere of He and nitrogen gases. By cooling the vapor-containing Ti atoms with He gas, Bentzon and Kragh[29] obtained ultrafine particles of TiN. They found that the only phase which could be observed by transmission electron microscopy is of the δ phase (fcc NaCl structure) and the dominating particle morphology was a cubic one with (100) surfaces. This is the same as the structures in Figs. 4 and 5. The finding certainly supports our assertion of the structure of the TiN cluster. In both cases, the TiN compounds grow from TiN molecules condensed in the gas phase.

The size of the large TiN clusters and those of the ultrafine particles are also comparable. For instance,

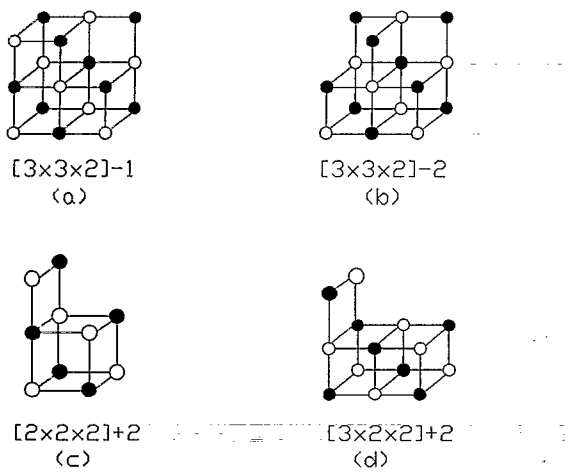

FIG. 6. Proposed structures of Ti_nN_{n-1} and Ti_nN_{n-2} cluster series, illustrated by examples: (a) $Ti_9N_8^+$; (b) $Ti_9N_7^+$; (c) $Ti_5N_5^+$; (d) $Ti_7N_7^+$. The solid circle represents the Ti atom and the open circle represents the N atom.

$Ti_{126}N_{126}$ [7×6×6] is already a small microcrystal with a size of about 2.5 nm, assuming the TiN bond length equal to the lattice parameter, $a=4.24$ Å.[30] Similarly, in Bentzon's experiment, the dominating crystal morphology is cubic with sizes ranging from 5 to 20 nm.

IV. CONCLUSIONS

In conclusion, $(TiN)_n^+$ clusters generated using a laser-induced plasma reactor source have been used to study the transition from the gas-phase cluster to the microcrystals of the condensed phase. There are a number of magic peaks in the mass spectra that indicate the special stability of clusters containing certain numbers of TiN molecules. These experimental results are the basis of the proposed geometry structures of these clusters. It has been shown that the fcc NaCl lattice structure actually occurs at the very early stages of clustering. Even very small sizes of TiN clusters evidently preferentially assemble into a cuboid structure.

The $(TiN)_n^+$ cluster series is a dominating one in the mass spectra. The concurrence of $(TiN)_n^+$, $Ti_nN_{n-1}^+$, and $Ti_nN_{n-2}^+$ suggests a fragmentation process upon multiphoton ionization. The geometry structures of $Ti_nN_{n-1}^+$ and $Ti_nN_{n-2}^+$ cluster series can be justified as microcrystal structures where one or two vacancies occur in the cubic lattices.

The transition-metal nitrides, carbides, and oxides produced with the laser-induced plasma reactor are very useful systems to study the molecular details of the change from the gaseous to the condensed state. These studies serve to bridge the gap between the isolated atom or molecule, and condensed matter. The investigations of other systems are now underway.

ACKNOWLEDGMENTS

Financial support from the U.S. Department of Energy, Grant No. DE-FGO2-92ER14258, is gratefully acknowledged. We thank Dr. B. Gou, B. May, and S. F. Cartier for help during the course of the work.

[1] A. W. Castleman, Jr. and R. G. Keesee, Chem. Rev. **86**, 589 (1986).
[2] A. W. Castleman, Jr. and R. G. Keesee, Acct. Chem. Res. **19**, 413 (1986).
[3] A. W. Castleman, Jr. and R. G. Keesee, Science **241**, 36 (1988).
[4] *Metal Clusters*, edited by F. Trager and G. zu Putlitz (Springer-Verlag, Berlin, 1986).
[5] *Elemental and Molecular Clusters*, edited by G. Benedek, T. P. Martin, and G. Pacchioni (Springer-Verlag, Berlin, 1987); W. A. de Heer, W. D. Knight, M. Y. Chou, and M. L. Cohen, *Solid State Physics*, edited by H. Ehrenreich, F. Seitz, and D. Turnbull (Academic, New York, 1987), Vol. 40, p. 93.
[6] *Ion and Cluster Ion Spectroscopy and Structure*, edited by J. P. Maier (Elsevier, New York, 1989).
[7] *Atomic and Molecular Clusters*, edited by E. R. Bernstein (Elsevier, New York, 1990).
[8] T. P. Martin, T. Bergmann, H. Gohlich, and T. Lange, J. Phys. Chem. **95**, 6423 (1991).
[9] T. P. Martin, Phys. Rep. **95**, 167 (1983).
[10] R. D. Beck, P. St. John, M. L. Homer, and R. L. Whetten, Science **253**, 879 (1990).
[11] E. C. Honea, M. L. Homer, and R. L. Whetten, Int. J. Mass Spectrom. Ion Proc. **102**, 213 (1990).
[12] J. Luo, U. Landman, and J. Jortner, in *Physics and Chemistry of Small Clusters*, edited by P. Jena, B. K. Rao, and S. N. Khanna (Plenum, New York, 1987), p. 201.
[13] G. Rajagopal, R. N. Barnett, and U. Landman, Phys. Rev. Lett. **67**, 727 (1991).
[14] P. J. Ziemann and A. W. Castleman, Jr., Phys. Rev. B **44**, 6488 (1991).
[15] P. J. Ziemann and A. W. Castleman, Jr., Z. Phys. D **20**, 97 (1991).
[16] P. J. Ziemann and A. W. Castleman, Jr., J. Chem. Phys. **94**, 718 (1991).
[17] *Structural of Inorganic Chemistry*, 4th ed., edited by A. F. Wells (Clarendon, Oxford, 1975).
[18] A. Neckel, in *The Physics and Chemistry of Carbides, Nitrides and Borides*, edited by R. Freer (Kluwer Academic, New York, 1990), p. 485.
[19] A. Harano, J. Kinoshita, and S. Koda, Chem. Phys. Lett. **172**, 219 (1990).
[20] B. C. Gou, S. Wei, Z. Y. Chen, J. Purnell, S. Buzza, K. P. Kerns, and A. W. Castleman, Jr., J. Chem. Phys. **97**, 5243 (1992).
[21] Z. Y. Chen, B. C. Gou, B. May S. Cartier, and A. W. Castleman, Jr., Chem. Phys. Lett. **198**, 118 (1992).
[22] *Periodic Table of The Elements* (Sargent-Welch Scientific, Skokie, IL, 1980).
[23] Z. Y. Chen, B. C. Gou, B. May S. F. Cartier, and A. W. Castleman, Jr. (unpublished).
[24] J. R. Heath, Y. Lin, S. C. O'Brien, Q.-L. Zhang, R. F. Curl, F. K. Tittel, and R. E. Smalley, J. Chem. Phys. **83**, 5520 (1985).
[25] T. G. Dietz, M. A. Duncan, D. E. Powers, and R. E. Smalley, J. Chem. Phys. **74**, 6511 (1981).
[26] W. C. Wiley and I. H. McLaren, Rev. Sci. Instrum. **26**, 1150 (1955).
[27] *Handbook of Chemistry and Physics*, 67th ed. (CRC, Boca Raton, 1986–1987), p. B227.
[28] R. Pflaum, K. Sattler, and E. Recknagel, in *Physics and Chemistry of Small Clusters*, edited by P. Jena, B. K. Rao, and S. N. Khanna (Plenum, New York, 1987), p. 103.
[29] M. D. Bentzon and F. Kragh, Z. Phys. D **19**, 299 (1991).
[30] *Inorganic and Organic Data Book*, Powder Diffraction File Set 38–1420, International Center for Diffraction Data, Philadelphia, PA, 1988, p. 533.